Available online at www.sciencedirect.com
SCIENCE DIRECT
Catalysis Today 99 (2005) 315–322
CATALYSIS TODAY
www.elsevier.com/locate/cattod

Adsorption and decomposition of H_2S on Pd(1 1 1) surface: a first-principles study

Dominic R. Alfonso[a,b,*], Anthony V. Cugini[a], Dan C. Sorescu[a]

[a]*National Energy Technology Laboratory, U.S. Department of Energy, P.O. Box 10940, 626 Cochrans Mill Road, Pittsburgh, PA 15236, USA*
[b]*Parsons Project Services, Inc., South Park, PA 15129, USA*

Available online 15 December 2004

Abstract

Gradient-corrected density functional theory was used to investigate the adsorption of H_2S on Pd(1 1 1) surface. Molecular adsorption was found to be stable with H_2S binding preferentially at top sites. In addition, the adsorption of other S moieties (SH and S) was investigated. SH and S were found to be preferentially bind at the bridge and fcc sites, respectively. The reaction pathways and energy profiles for H_2S decomposition giving rise to adsorbed S and H were determined. Both $H_2S_{(ad)} \rightarrow SH_{(ad)} + H_{(ad)}$ and $SH_{(ad)} \rightarrow S_{(ad)} + H_{(ad)}$ reactions were found to have low barriers and high exothermicities. This reveals that the decomposition of H_2S on Pd(1 1 1) surface is a facile process.

Keywords: Density functional calculations; Dissociative adsorption; Chemisorption; Palladium; Hydrogen sulfide; Sulfuhydryl species (SH); Sulfur; Metallic surface; Low index single crystal surface

1. Introduction

Hydrogen is being touted as a potential fuel of the future. It is the fuel of choice for low-temperature fuel cells which function by converting the energy released from the oxidation of hydrogen into electrical power. A particular promising technology for the production of hydrogen is coal gasification [1–3]. When heated in a controlled atmosphere, coal produces primarily synthesis gas (a mixture of H_2, CO and other hydrocarbons). Synthesis gas can be further processed using a gas-shift reactor technology to produce more hydrogen. Hydrogen could then be separated from carbon dioxide and other contaminants using palladium membrane based purification technique [4–6]. Non-porous inorganic membranes made from palladium have long been of interest because of their capabilities to separate hydrogen at ppb impurity levels. However, sulfur poisoning has been found to have negative effects on the performance of these materials [7–10]. It has been reported that even the presence of a small amount of sulfur compounds in the feeds can lead to deactivation of these materials after prolonged operation [11,12]. Uncontrollable and accidental poisoning of sulfur can be a considerable financial burden and it has been reported that millions of dollars are lost every year in the chemical industries as a result of sulfur poisoning [13].

The generation of a sulfided Pd(1 1 1) surface using H_2S as a carrier gas has drawn considerable interest in recent years [14–18]. H_2S is one of the most common impurities in fossil fuel based feed streams. Consequently, the behavior of H_2S on palladium represents a prototype model for understanding the various reasons for the poisoning of palladium by sulfur compounds. Palladium reacts readily with H_2S and become partially covered with sulfur adatoms, which are considered as the true poisons. On Pd(1 1 1) surface, the existence of adsorbed sulfur with a variety of structures was detected from LEED, STM, XPS and AES studies [14–18]. Coexisting $\sqrt{3} \times \sqrt{3}\,R30^\circ$ and 2×2 structures were found at room temperature. The formation of $\sqrt{7} \times \sqrt{7}\,R19^\circ$ was favored when the surface was annealed above 700 K. The observed poisoning of palladium was ascribed to site blocking by adsorbed sulfur atoms, which form strong covalent bonds with the metal atoms [13,19,20]. The formation of strong covalent bonds between the sulfur and the substrate was attributed to the substantial overlap of sulfur p-states with the metal surface d-band

* Corresponding author. Tel.: +1 412 386-4113; fax: +1 412 3865920.
E-mail address: alfonso@netl.doe.gov (D.R. Alfonso).

0920-5861/$ – see front matter
doi:10.1016/j.cattod.2004.10.006

[13,19,20]. The formation of sulfur-covered metal surface affects the dissociation and diffusion rates for hydrogen leading to reduction in hydrogen permeation through palladium membranes [21,22].

Clearly, the effect of H_2S adsorption is the deposition of sulfur on the surface, which represents the true poison. Therefore, the adsorption of H_2S and its decomposition on palladium are important steps in the poisoning process. Improved insight into the fundamental mechanism is important for development of materials that either resist sulfur poisoning or adsorb a limited amount of sulfur compounds, without drastically inhibiting their chemical activity. Despite the importance of this problem, the literature appears to lack a detailed atomic level description of the surface chemistry of H_2S on Pd(1 1 1) surfaces. In addition to sulfur, adsorbed hydrogen was also found on Pd(1 1 1) surface after exposing it to H_2S at room temperature [14]. Moreover, as shown below, sulfuhydryl (SH) species bind on the Pd(1 1 1) surface. These facts suggest that H_2S decomposition via sequential S–H scission on Pd(1 1 1) surface might deserve a thorough study.

The objective of this paper is to present first-principles density functional theory calculations of the energetics of H_2S adsorption and its decomposition pathway on the Pd(1 1 1) surface. We present here results on the binding energy and the corresponding optimized adsorption configurations of molecularly adsorbed H_2S on Pd(1 1 1) surface. In addition, the adsorption of the corresponding S-containing dissociated species (S and SH) was also investigated. The study of decomposition pathways related to S–H bond breaking on the surface including thermochemistry and reaction barriers will be addressed. The paper is organized as follows. The technical details of the calculations are outlined in Section 2. In Section 3, we describe and discuss the results and place them in a wider context. Our conclusions are drawn in the final section (Section 4).

2. Calculation details

The calculations were performed using spin-polarized periodic density functional theory (DFT) as implemented in the Vienna ab initio simulation package (VASP) [23,24]. The Kohn–Sham equations were solved iteratively using residuum-minimization techniques and optimized charge-density mixing schemes. Ionic cores were described by non-local reciprocal space ultra soft pseudo-potentials in the Vanderbilt form [25,26]. The Kohn–Sham one-electron valence states were expanded in a plane-wave basis set. The exchange-correlation energy was described at the level of generalized gradient approximation (GGA) in the implementation of Perdew and coworkers (PW91) [27,28].

In order to model the Pd(1 1 1) surface, we used a periodic supercell. First the bulk Pd was geometrically optimized in order to determine the equilibrium lattice constant. After optimization of the bulk fcc crystal, the (1 1 1) surface was generated by construction of a three-dimensional periodic supercell composed of three metal layers. The slab model was separated by 12 Å of vacuum space. In the present study, we limit our analysis to the case of small coverages (0.06 ML $< \theta <$ 0.33 ML). The higher coverage regime will be considered in future work. Adsorption of H_2S, SH and S at $\theta = 0.06$ ML was investigated by placing the respective adsorbate on one side of a 4×4 surface unit cell. Adsorption at $\theta = 0.11$, 0.22 and 0.33 ML was studied using a 3×3 surface unit cell containing one, two and three adsorbates on the free surface, respectively.

All the atoms in the slab model except the bottom layer were allowed to relax. The geometrical optimizations were done using a quasi-Newton optimization scheme and the structural parameters were considered as converged when the atomic forces were less than 0.03 eV/Å. For the Brillouin zone integrations, a $3 \times 3 \times 1$ Monkorst-Pack k-point grid [29] was used. A Methfessel–Paxton smearing [30] of $\sigma = 0.2$ eV was utilized and the corrected energy for $\sigma \rightarrow 0$ was employed. A cutoff energy of 234 eV was used in the expansion of the plane wave basis set.

The binding energy of the adsorbate species, E_{bind}, was calculated with the formula:

$$E_{\text{bind}} = E_{\text{adsorbate+slab}} - (E_{\text{adsorbate}} + E_{\text{slab}}) \quad (1)$$

where $E_{\text{adsorbate + slab}}$ is the total energy of the relaxed adsorbate-surface system, while E_{slab} and $E_{\text{adsorbate}}$ are the total energy of the relaxed bare surface and gas phase adsorbate, respectively. Hence, the binding energy is defined as negative if the total energy decreases when the adsorbate is brought from infinity and placed onto the surface. The overall reaction energy, ΔE_{rxn} was calculated using the expression

$$\Delta E_{\text{rxn}} = \sum E_{\text{prod}} - \sum E_{\text{react}} \quad (2)$$

where the first and second terms represent the sum of energies of products and reactants, respectively. Based on this convention, negative reaction energy corresponds to an exothermic reaction.

Our calculated lattice constant for bulk Pd is 3.965 Å, in excellent agreement with experimental data (3.883 Å [31]). The equilibrium geometry of H_2S and SH molecules was also computed. The molecules were optimized in a large cell of 15 Å × 15 Å × 15 Å. Comparison of our calculated structural parameters with previous theoretical predictions and experimental data confirms that these molecules are described accurately by the present methods. The bond length and bond angle of H_2S molecule were found to be 1.348 Å and 92.8°, respectively, in excellent agreement with the corresponding experimental values of 1.328 Å and 92.2° [32]. Similarly, the computed bond length of SH is 1.352 Å, which is in excellent agreement with the experimental value of 1.345 Å [32].

The dissociation of H_2S was studied by placing the molecule on one side of the 4×4 surface unit cell. We

employed the nudged elastic band (NEB) technique [33,34] to map out the minimum energy path for the decomposition process. The NEB method employs a discrete representation of the reaction path, with the points (images) along the path being relaxed using first derivative information only. In this work, an initial chain of images is constructed between the initial reactants and final reaction products using linear interpolation between the two endpoints. These images were relaxed simultaneously (with additional elastic forces) using quasi-Newton optimization scheme until the projected forces were below 0.08 eV/Å. In order to obtain a better estimate of the transition state structures, the highest energy images from the NEB calculations were optimized further until the forces on the systems were below 0.03 eV/Å.

3. Results and discussion

3.1. Adsorption of sulfur-containing species

3.1.1. Hydrogen sulfide (H_2S) adsorption on Pd(1 1 1)

H_2S can interact in several different ways with the surface of a metal like Pd. A detailed account of the binding modes of H_2S will be presented elsewhere. Here we consider only the results corresponding to the most stable configuration. For H_2S, adsorption occurs through a bond between the sulfur atom of H_2S and a nine-fold coordinated surface metal atom (top site adsorption, see Fig. 1a). In this configuration, H_2S lies nearly parallel to the surface, the angle between the adsorbate plane and the surface being $\sim 10^{\circ}$. The calculated S–Pd distance is 2.37 Å. One S–H bond is directed toward an hcp site whereas the other one points towards a bridge site. Relative to the relaxed clean surface, the surface atom which sulfur is bonded to moves out by 0.14 Å. The predicted binding energy in the low coverage limit is −0.71 eV with respect to gas phase H_2S.

H_2S adsorption was also examined at higher coverages ranging from 0.11 to 0.33 ML (Figs. 1b–d). The energetic and geometrical parameters at different coverages are tabulated in Table 1. It can be seen that the binding energies are essentially similar for coverage 0.06 and 0.11 ML. Above 0.11 ML, the binding energies slightly decrease with increasing coverage indicating that a small repulsive interaction between adsorbates builds up. We note that the overall variation in the magnitude of the adsorption energy is rather small, i.e. not greater than ∼0.07 eV. Additionally, the structural properties of the adsorbed H_2S did not change appreciably for the 0.06–0.33 ML coverage range considered.

There are a number of experimental studies on sulfided Pd(1 1 1) obtained through H_2S decomposition [14,15,17]. It was found that at room temperature, H_2S dissociates quickly on Pd(1 1 1) surface giving rise to adsorbed S species. Since the main focus of these studies was to analyze the structure of the adsorbed sulfur, no details have been provided regarding the adsorbed H_2S species. Our work, to our knowledge, provides the first direct theoretical confirmation that molecular adsorption of H_2S on Pd(1 1 1) is energetically favorable.

3.1.2. Sulfuhydryl (SH) adsorption on Pd(1 1 1)

Sulfuhydryl is extremely unstable and a short-lived intermediate. To our knowledge, the existence of this species on Pd(1 1 1) has not yet been observed and characterized experimentally. Therefore, a theoretical approach is particularly useful for providing important information on the

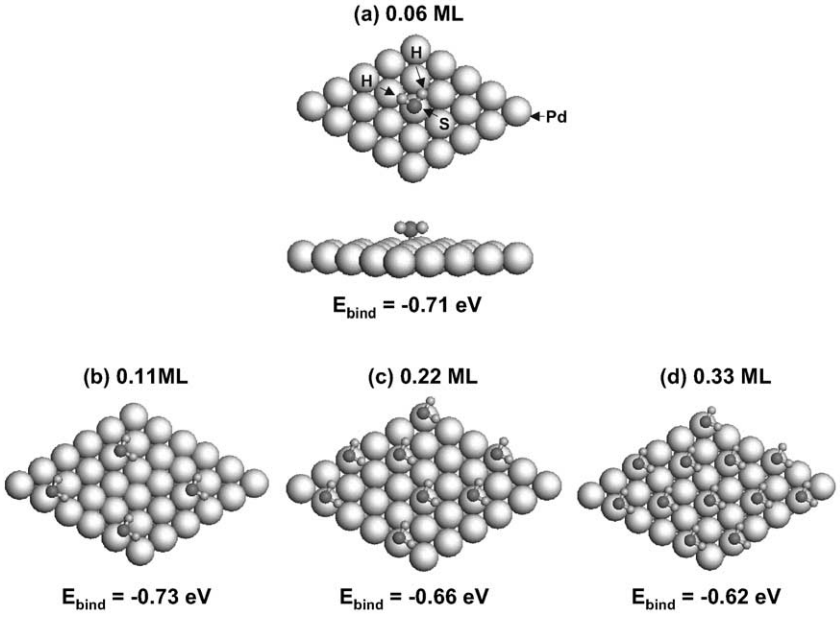

Fig. 1. Adsorption configuration of H_2S at the top sites of Pd(1 1 1) surface at coverages (a) 0.06 ML, (b) 0.11 ML, (c) 0.22 ML and (d) 0.33 ML.

Table 1
Binding energies and optimized structural parameters for the adsorption of H_2S at the top site of Pd(1 1 1) at different coverages. The calculated structural properties of the gas phase H_2S are included for comparison

θ (ML)	E_{bind} (eV)	r (S–Pd) (Å)	r (S–H) (Å)	(Pd–S–H) (°)	(H–S–H) (°)
0.06	−0.71	2.37	1.36	101.5	91.6
0.11	−0.73	2.34	1.37	100.0	91.7
0.22	−0.66	2.34	1.37	100.5	91.6
0.33	−0.62	2.33	1.37	99.0	91.4
$H_2S_{(g)}$			1.35		92.8

structure and energetics of adsorption of this species. As in the case of H_2S adsorption, here we consider only results corresponding to the most stable configuration identified on the surface. Fig. 2a displays the most stable structure of SH on Pd(1 1 1) surface in the low coverage limit. SH was found to preferentially bind at a bridge site. The calculated S–Pd and S–H bond distances are 2.32 and 1.39 Å, respectively. The S–H axis is inclined by ∼21° from the surface plane. Relative to the relaxed clean surface, the surface atom, which the sulfur is bonded to moves out by 0.06 Å. The calculated binding energy for SH on the surface is −3.02 eV with respect to gas phase SH.

The energetics and structures of SH at the bridge sites for higher coverages 0.11, 0.22 and 0.33 ML are tabulated in Table 2 (also see Fig. 2b–d). From 0.06 to 0.11 ML there is a slight enhancement in the adsorption energy. The S–H bond length tends to be slightly elongated at the 0.11 ML coverage compared to the 0.06 ML coverage case (1.44 Å versus 1.39 Å) which indicates that the increase in the binding energy may be due to enhanced H-bonding interactions between neighboring SH groups. Above 0.11 ML, the binding energies slightly decrease with increasing coverage, which is an indication that a small repulsive interaction between adsorbates starts to build up.

Table 2
Binding energies and optimized structural parameters for the adsorption of SH at the bridge site of Pd(1 1 1) at different coverages. The calculated structure of gas phase SH is included for comparison

θ (ML)	E_{bind} (eV)	r (S–Pd) (Å)	r (S–H) (Å)	(Pd–S–H) (°)
0.06	−3.02	2.32	1.39	104.4
0.11	−3.07	2.32	1.44	104.8
0.22	−3.00	2.33	1.41	101.3
0.33	−2.97	2.33	1.40	99.6
$SH_{(g)}$			1.35	

3.1.3. Sulfur adsorption on Pd(1 1 1)

We found that the most stable adsorption configuration of sulfur corresponds to adsorption at the three-fold hollow fcc site in agreement with previous studies [13,19,20]. In the low coverage limit (Fig. 3a), the binding energy is −5.15 eV with respect to atomic S. The calculated S–Pd distance is 2.27 Å. We find that the binding on the other type of hollow site (hcp) is slightly lower by 0.08 eV. The predicted binding energies at higher coverages (Fig. 3b–d) are tabulated in Table 3. These results indicate that binding energy decreases with increasing coverage. This trend was also observed in the DFT studies of Toulhoat and coworkers [19] for S

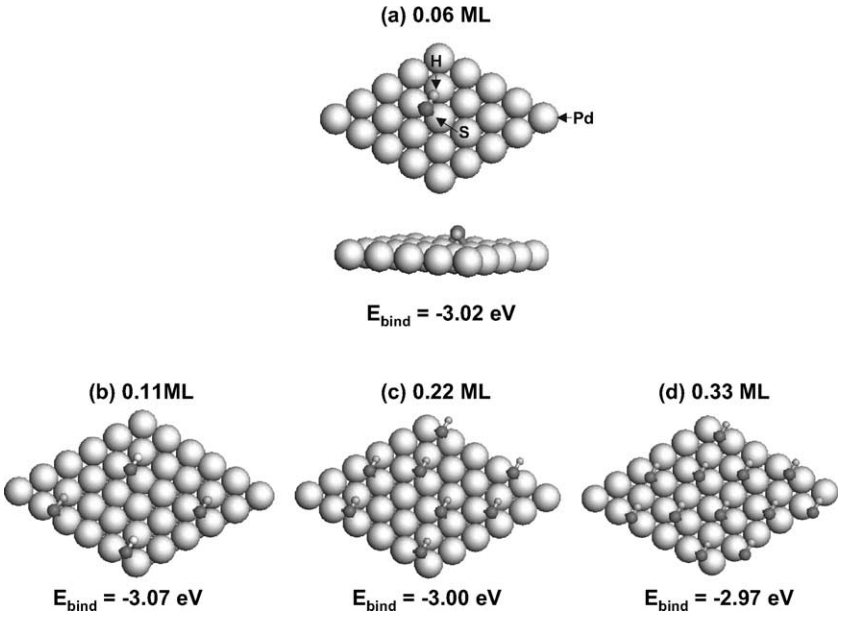

Fig. 2. Adsorption configuration of SH at the bridge sites of Pd(1 1 1) surface at coverages (a) 0.06 ML, (b) 0.11 ML, (c) 0.22 ML and (d) 0.33 ML.

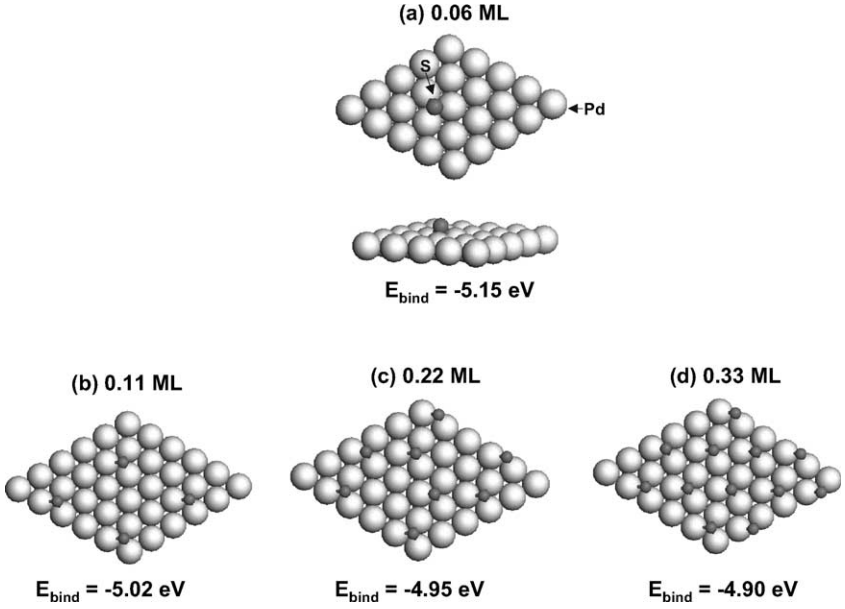

Fig. 3. Adsorption configuration of S at the fcc sites of Pd(1 1 1) surface at coverages (a) 0.06 ML, (b) 0.11 ML, (c) 0.22 ML and (d) 0.33 ML.

adsorbed on Pd(1 1 1) surface. They attributed the observed trend to the repulsive nature of the S–S interactions.

The sulfur–metal distances observed in our calculations for Pd(1 1 1) are found in the range 2.26–2.27 Å. These values are comparable to those obtained from LEED studies for a $\sqrt{3} \times \sqrt{3}\,R30^\circ$ S adlayer on Pd(1 1 1) (2.23–2.28 Å) [18]. Very similar bond lengths were reported by Rodriguez et al. using ab initio SCF calculations with a 12 atom cluster model of Pd(1 1 1) [35]. The adsorption energies predicted for atomic sulfur with values between −4.90 and −5.15 eV indicate the existence of a strong S–Pd interaction. These results are also consistent with the experimental observations that S adatoms remain on the surface even for temperatures in excess of 800 K [14,15,17].

3.2. Adsorption of hydrogen

The most favorable binding site for H on Pd(1 1 1) surface is found to be at the fcc site. The predicted H–Pd distance is 1.82 Å. Relative to the relaxed clean surface, the three surface atoms, which the H is bonded to moves out by 0.07 Å. The binding energy on the fcc site is −0.60 eV with respect to gas phase H_2. The binding energy on the corresponding hcp site is about 0.04 eV lower in energy than the fcc site. Our findings for the H adsorption are in very good agreement with previous LEED studies of van Hove and coworkers [36]. They found that the fcc site is the most favorable binding site for H on Pd(1 1 1) with measured H–Pd bond lengths in the range 1.78–1.80 Å. Previous DFT calculations also identified the fcc hollow site as the most stable [37–39]. Additionally, the predicted energy barrier for diffusion between adjacent three-fold hollow sites (via the bridge site) is 0.11 eV. This indicates that hydrogen diffusion barrier is small in agreement with previous theoretical and experimental studies [37–39].

Table 3
Binding energies and optimized structural parameters for the adsorption of S at the fcc site of Pd(1 1 1) at different coverages

θ (ML)	E_{bind} (eV)	r (S–Pd) (Å)
0.06	−5.15	2.27
0.11	−5.02	2.27
0.22	−4.95	2.26
0.33	−4.90	2.26

3.3. Dissociative reactions

The reaction pathways for adsorption of H_2S from the gas phase as well as the dissociation of H_2S on Pd(1 1 1) were studied theoretically using the NEB method. For this purpose, we considered the following processes:

$$H_2S_{(gas)} \rightarrow H_2S_{(ad)},$$

$$H_2S_{(ad)} \rightarrow SH_{(ad)} + H_{(ad)},$$

$$SH_{(ad)} \rightarrow S_{(ad)} + H_{(ad)}.$$

3.3.1. Adsorption of H_2S from the gas phase: $H_2S_{(gas)} \rightarrow H_2S_{(ad)}$

We first determined the reaction pathway for molecular adsorption of H_2S from the gaseous phase. For the initial state, the H_2S molecule is placed about 3.6 Å above a surface atom on Pd(1 1 1). The final state of this process corresponds to a H_2S molecule adsorbed at the top site. The calculated reaction energy for this process is found to be $\Delta E_{rxn} = -0.71$ eV which is equal to the adsorption energy of H_2S. Our results show that there is no barrier to

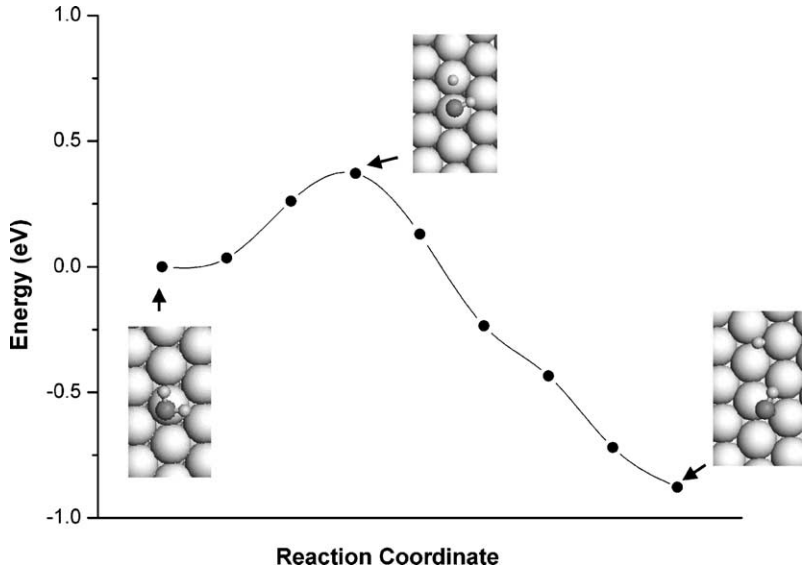

Fig. 4. The minimum energy path for the abstraction of a hydrogen atom from H_2S on Pd(1 1 1) surface.

adsorption, indicating that the molecular adsorption of H_2S is a non-activated process.

3.3.2. First dissociation step: $H_2S_{(ad)} \rightarrow SH_{(ad)} + H_{(ad)}$

We then calculated the reaction pathway for the cleavage of sulfuhydryl hydrogen starting from the molecularly adsorbed H_2S ($H_2S_{(ad)} \rightarrow SH_{(ad)} + H_{(ad)}$). The initial state of this elementary reaction step corresponds to a H_2S molecule adsorbed at the top site of the surface. The final state corresponds to SH and H adsorbed in their most stable configuration (i. e., SH is at the bridge site and the H atom is at the fcc site). The calculated reaction pathway for $H_2S_{(ad)} \rightarrow SH_{(ad)} + H_{(ad)}$ is presented in Fig. 4.

We found that this process is energetically favorable on Pd(1 1 1) surface and the overall predicted energy change for this reaction step is $\Delta E_{rxn} = -0.88$ eV. On Pd(1 1 1) surface, the dissociating H initially moves towards an adjacent surface atom and eventually ends up in a three-fold fcc site. As the H_2S molecule comes apart, the SH fragment tilts toward the surface and ends in a bridge configuration with the S–H bond directed toward a top site. At the transition state of the reaction (see Fig. 4), both SH and H are close to adjacent top sites with the dissociating H, 2.55 Å away from the S atom of the SH fragment. We note that the dissociating H is practically abstracted from the SH fragment. In the transition state, the S–metal bond lengths are about 2.28 Å. The values are reduced by 0.09 Å compared to the molecularly adsorbed H_2S. After the transition state, the SH fragment moves toward a two-fold bridge site with S–metal bond length of 2.32 Å. The computed S–H bond length in the transition state has a value of 1.38 Å. This value is intermediate between the gas phase value of 1.345 Å and that obtained for the adsorbed species of 1.40 Å. The computed energy barrier for the hydrogen abstraction is found to be 0.37 eV.

We also examined the case of adsorption of SH and H species on Pd(1 1 1) in separate 4×4 surface unit cells. Our calculations reveal that there is practically no energy gained when SH and H are adsorbed in the same 4×4 supercell or in separate supercells. This implies that there is practically no lateral interaction between SH and H for the configurations we investigated.

3.3.3. Second dissociation step: $SH_{(ad)} \rightarrow S_{(ad)} + H_{(ad)}$

We calculated the minimum energy pathway for the abstraction of H from the adsorbed SH giving rise to adsorbed S and H species ($SH_{(ad)} \rightarrow S_{(ad)} + H_{(ad)}$). The corresponding result is shown in Fig. 5. The initial state for this elementary reaction step is SH adsorbed at the bridge site of the Pd(1 1 1) surface. The final state corresponds to S and H adsorbed at the fcc sites. As with the first dissociation step, this process is also predicted to be exothermic. The energy change for this reaction step is $\Delta E_{rxn} = -0.73$ eV. The dissociating H initially moves towards an adjacent surface atom and eventually ends up in a three-fold fcc site. As the SH molecule comes apart, the S fragment tilts toward the surface and ends on fcc site.

The barrier for the second S–H cleavage is very small (~0.04 eV) suggesting that this is nearly a spontaneous process. The SH fragment in the transition state configuration closely resembles the chemisorbed SH species. In this case, the S–H bond is slightly modified by about 9% relative to the equilibrium bond distance of adsorbed SH (1.39 Å). After passing the transition state, the distance between S and the dissociating H progressively increases as both atoms come apart and move towards fcc sites.

The separate adsorptions of S and H atoms in separate 4×4 unit cells were also investigated. As with the coadsorption of SH and H, we find that for the configurations considered there is practically no lateral interaction between

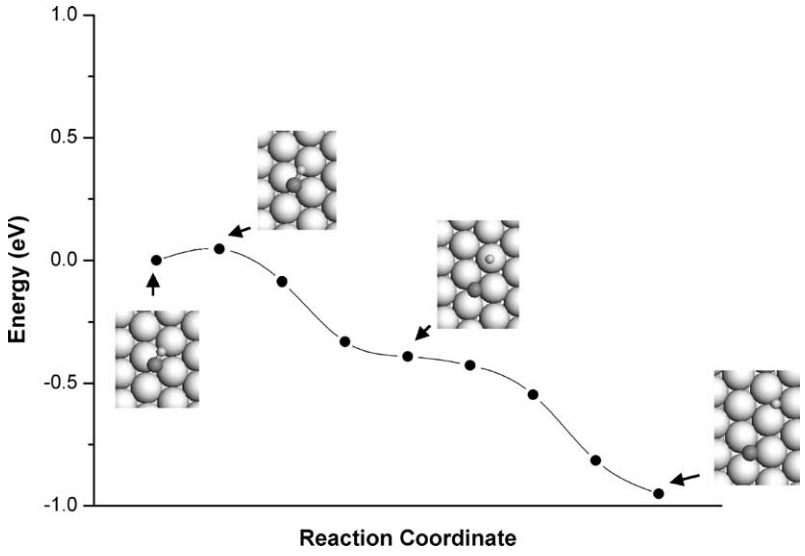

Fig. 5. The minimum energy path for the abstraction of a hydrogen atom from SH on Pd(1 1 1) surface.

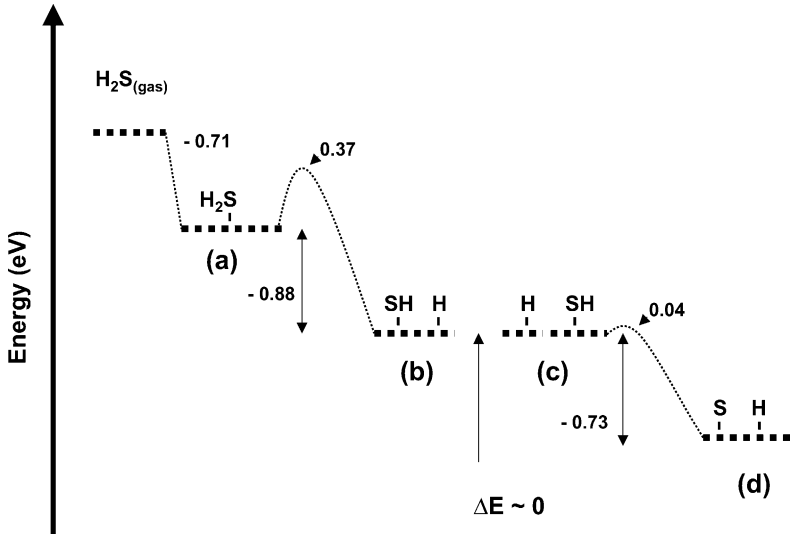

Fig. 6. Relative energy diagram for H_2S adsorption and decomposition on Pd(1 1 1) surface in a 4 × 4 unit cell. The states labeled with (a), (b) and (d) correspond to adsorbed H_2S, dissociated H_2S and dissociated SH, respectively. The state labeled (c) corresponds to SH and H chemisorbed in separate 4 × 4 surface unit cells. ΔE notation indicates that there is practically no energetic difference between states (a) and (b).

S and H. The calculated stability of the coadsorbed state is comparable to the case when S and H are adsorbed in separate surface unit cells.

Fig. 6 reveals the detailed energy profile for the adsorption and decomposition of H_2S on Pd(1 1 1). As mentioned previously, H_2S adsorption from the gas phase is non-activated and exothermic. Additionally, both $H_2S_{(ad)} \rightarrow SH_{(ad)} + H_{(ad)}$ and $SH_{(ad)} \rightarrow S_{(ad)} + H_{(ad)}$ reactions have low barriers and high exothermicities. As a result, the decomposition of H_2S upon adsorption from the gas phase is predicted to be a facile process. We note that because the chemisorption and dissociation properties of H_2S on Pd(1 1 1) surface have not yet been studied experimentally, a direct comparison to our calculations is not possible. Nonetheless, our findings are consistent with experiments which find that H_2S is not stable on the clean Pd(1 1 1) surface at room temperature [14,15,17]. In these studies, sulfidation of Pd(1 1 1) has been obtained with H_2S as a carrier gas. In general, S adsorbed on Pd(1 1 1) was found after adsorption of H_2S at room temperature, suggesting that S–H bonds cleaves at this temperature. Our predicted activation energies for S–H cleavage on Pd(1 1 1) have small values (<0.4 eV). These findings explain qualitatively the low temperature observed for dissociation.

4. Conclusions

Gradient-corrected Density Functional Theory was employed to investigate the molecular and dissociative adsorption of H_2S on the clean Pd(1 1 1) surface. We

identified stable adsorption structures and binding energies for H_2S, SH and S species. For H_2S, we find that molecular adsorption is energetically favorable with the adsorbate binding preferentially at top sites. SH and S bind preferentially at the bridge sites and fcc sites, respectively. Additionally, minimum energy pathways and energy profiles for the decomposition of H_2S into adsorbed S and H were determined. Our calculations indicate that H_2S adsorption from the gas phase is non-activated and exothermic. The dissociative adsorption of H_2S is exothermic and the calculated activation energies are relatively small ($<$0.4 eV). This reveals that adsorbed H_2S on Pd(1 1 1) is unstable and its decomposition on the Pd(1 1 1) is a facile process.

References

[1] S. Lin, M. Harada, Y. Suzuki, H. Hatano, Fuel 81 (2002) 2079.
[2] C. Fushimi, M. Goto, A. Tsutsumi, J. Hayashi, T. Chiba, J. Anal. Appl. Pyrolysis 70 (2003) 185.
[3] T.A. Czuppon, S.A. Knez, D.S. Newsome, in: A. Bisio, S. Boots (Eds.), Encyclopedia of Energy Technology and Environment, John Wiley & Sons, New York, 1995, p. 1752.
[4] R.E. Buxbaum, Sep. Sci. Technol. 34 (1999) 2113.
[5] Y.M. Lin, G.-L. Lee, M.H. Rei, Catal. Today 44 (1998) 343.
[6] K. Aasberg-Petersen, C.S. Nielsen, S.L. Jorgensen, Catal. Today 46 (1998) 193.
[7] M.L. Burke, R.J. Madix, Surf. Sci. 237 (1990) 1.
[8] R.V. Bucur, J. Catal. 70 (1981) 92.
[9] C.H.F. Peden, B.D. Kay, D.W. Goodman, Surf. Sci. 175 (1986) 215.
[10] F.J. Castro, G. Meyer, G. Zampieri, J. Alloy Compd. 330-332 (2002) 612.
[11] J. Lee, H. Rhee, J. Catal. 177 (1998) 208.
[12] J. Oudar, H. Wise, Deactivation and Poisoning of Catalysts, Dekker, New York, 1991.
[13] J.A. Rodriguez, J. Hrbek, Acc. Chem. Res. 32 (1999) 719.
[14] S. Speller, T. Rauch, J. Bömermann, P. Bormann, W. Heiland, Surf. Sci. 441 (1999) 107.
[15] V.R. Dhanak, A.G. Shard, B.C.C. Cowie, A. Santoni, Surf. Sci. 410 (1998) 321.
[16] F. Maca, M. Scheffler, W. Berndt, Surf. Sci. 160 (1985) 467.
[17] J.G. Forbes, A.J. Gellmann, J.C. Dunphy, M. Salmeron, Surf. Sci. 279 (1992) 68.
[18] M.E. Grillo, C. Stampfl, W. Berndt. Surf. Sci. 317 (1994) 84.
[19] P.A. Gravil, H. Toulhoat, Surf. Sci. 430 (1999) 176.
[20] D.R. Alfonso, A.V. Cugini, D.S. Sholl, Surf. Sci. 546 (2003) 12.
[21] S. Wilke, M. Scheffler, Surf. Sci. 329 (1995) 605.
[22] S. Wilke, M. Scheffler, Phys. Rev. Lett. 76 (1996) 3380.
[23] G. Kresse, J. Hafner, Phys. Rev. B 47 (1993) 558.
[24] G. Kresse, F.J. Furthmüller, Comp. Mat. Sci. 6 (1996) 15.
[25] D.H. Vanderbilt, Phys. Rev. B 41 (1990) 7892.
[26] G. Kresse, J. Hafner, J. Phys. Condens. Matter. 6 (1994) 8245.
[27] J.P. Perdew, Y. Wang, Phys. Rev. B 33 (1986) 8800.
[28] J.P. Perdew, J.A. Chevary, S.H. Vosko, K.A. Jackson, M. Pederson, D.J. Singh, C. Fiolhais, Phys. Rev. B 46 (1992) 6671.
[29] H.J. Monkhorst, J.D. Pack, Phys. Rev. B 13 (1976) 5188.
[30] M. Methfessel, A. Paxton, Phys. Rev. B 40 (1989) 3616.
[31] B.R. Coles, J. Inst. Met. 84 (1956) 346.
[32] J.M.W. Chase, NIST-JANAF Thermochemical Tables, Hemisphere, New York, 1989.
[33] G. Mills, H. Jönsson, G. Schenter, Surf. Sci. 324 (1995) 305.
[34] G. Henkelman, B.P. Uberuaga, H. Jönsson, J. Chem. Phys. 113 (2000) 9901.
[35] J.A. Rodriguez, S. Chatuvedi, T. Jirsak, Chem. Phys. Lett. 296 (1998) 421.
[36] T.E. Felter, E.C. Sowa, M.A. van Hove, Phys. Rev. B 40 (1989) 891.
[37] W. Dong, V. Ledentu, P. Sautet, A. Eichler, J. Hafner, Surf. Sci. 411 (1998) 123.
[38] J.F. Paul, P. Sautet, Surf. Sci. 356 (1996) 403.
[39] G.W. Watson, R.P.K. Wells, D.J. Willock, G.J. Hutchings, J. Phys. Chem. B 105 (2001) 4889.